

It seems unlikely that the discrepancy at high primary energies can be attributed to a poor approximation to the escape function since in this energy region the yield is determined mainly by the production of secondaries. Better agreement might be obtained for Ge by use of a smaller value for the exponent n , but, as mentioned above, this alone is not adequate for MgO. The origin of the difficulty appears to reside in two approximations used: (a) a mean energy of formation for the secondary electrons which is independent of the primary energy, and (b) a uniform production throughout the range of the primary beam. The first of these would not be expected to hold true over a wide range of energies, and with reference to (b) it should be noted that deviations are expected at high energies on the basis of Young's results.

In conclusion one might say that the modifications of the elementary theory introduced above provide considerably better agreement between the theoretical and experimental reduced yield curves. However, the experimental data show that there does not exist a

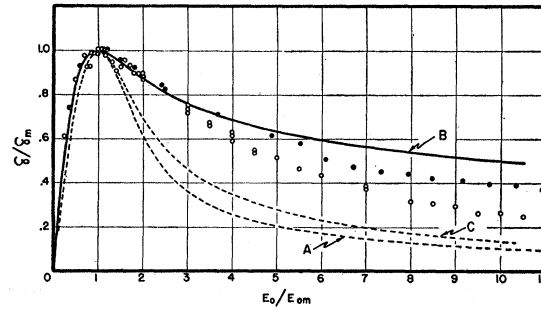


FIG. 6. Curve A represents Eq. (2). Curves B and C represent expression (17) for $n=0.35$ and $n=1.0$, respectively. The open circles are data for the MgO crystal shown by solid circles in Fig. 5, extended to a primary energy of 10.5 kev. The solid circles represent data for a germanium crystal obtained by Johnson and McKay, reference 12.

reduced yield curve which is common to all materials. Variations of the reduced yield curve from one material to another evidently require more detailed considerations of the production and escape mechanisms.

Oscillatory Galvanomagnetic Properties of Bismuth Single Crystals in Longitudinal Magnetic Fields*

JULIUS BABISKIN

United States Naval Research Laboratory, Washington, D. C., and The Catholic University of America, Washington, D. C.

(Received April 18, 1957)

The galvanomagnetic effects of oriented single crystals of bismuth have been studied in longitudinal magnetic fields up to 60 000 gauss at liquid helium temperatures. Oscillatory behaviors with de Haas-van Alphen periodicity were discovered to be superimposed upon the normal galvanomagnetic effects. These results showed that the periods for galvanomagnetic oscillations were independent of the direction and magnitude of the electric current. At high fields, a previously unreported oscillation was observed having a period which compares favorably with the period calculated from parameters for the de Haas-van Alphen effect at the same orientation. At the higher fields and lower temperatures, the galvanomagnetic oscillations exhibited a remarkable resemblance to the exact theory for the oscillatory magnetic susceptibility of a free-electron gas. Both the normal and the oscillatory galvanomagnetic effects are analyzed in terms of a tilted, multi-ellipsoidal model. For one of the orientations studied, the normal longitudinal magnetoresistance exhibited an anomalous maximum, which is attributed to scattering from internal surfaces.

INTRODUCTION AND THEORY

THIS paper has a twofold purpose in that two classes of phenomena, which occur simultaneously in these experiments, are studied. These are: (a) the normal galvanomagnetic effects of oriented single crystals of bismuth in longitudinal magnetic fields (H_L), and (b) the oscillatory galvanomagnetic effects with de Haas-van Alphen periodicity which were observed to be superimposed upon these normal galvanomagnetic effects. These measurements were taken in H_L up to 60 000 gauss and mainly at liquid helium temperatures.

* Based on a dissertation submitted to the Faculty of the Graduate School of The Catholic University of America in partial fulfillment of the requirements for the degree of Doctor of Philosophy.

The normal galvanomagnetic effects of anisotropic single-crystal specimens can be classified¹ into the four following cases:

(a) Longitudinal effects in transverse magnetic fields (H_T) or the transverse magnetoresistance. In this case, $\mathbf{H} \perp \mathbf{J} \parallel \mathbf{E}$ where \mathbf{H} is the applied magnetic field, \mathbf{J} is the electric current, and \mathbf{E} is the measured component of the electric field.

(b) Transverse effects in H_T or the Hall effect ($\mathbf{H} \perp \mathbf{J} \perp \mathbf{E} \perp \mathbf{H}$).

(c) Longitudinal effects in H_L or the longitudinal magnetoresistance ($\mathbf{H} \parallel \mathbf{J} \parallel \mathbf{E}$).

¹ A. H. Wilson, *Theory of Metals* (Cambridge University Press, London, 1953), p. 209.

(d) Transverse effects in H_L ($\mathbf{H} \parallel \mathbf{J} \perp \mathbf{E}$), which have been observed experimentally but have no common name.

These effects are generally measured with \mathbf{J} parallel to the specimen length. Since some or all of the above effects can exist at all orientations of the crystal, these effects are generally measured, for simplicity, with each of \mathbf{J} , \mathbf{E} , and \mathbf{H} aligned parallel or perpendicular with respect to the axes of crystal symmetry, which in turn have a preferred orientation with respect to the geometry of the specimen. If \mathbf{J} , \mathbf{E} , \mathbf{H} , the specimen length and the axes of crystal symmetry are aligned arbitrarily with respect to each other at angles other than 0° or 90° (e.g., due to imperfect alignment), then the measured effect will be some combination of the above effects. In order to avoid size effects, the specimen dimensions are made large compared to the electronic mean free path.

The major emphasis of this paper is directed towards the study of the oscillatory galvanomagnetic effects in H_L which had not been previously observed. In 1930, Schubnikow and de Haas² discovered that the transverse magnetoresistance of bismuth exhibited a magneto-oscillatory dependence at low temperatures. This discovery led de Haas and van Alphen³ to the observance of a magneto-oscillatory behavior for the magnetic susceptibility of bismuth, which is commonly called the de Haas-van Alphen effect.

The theory of the de Haas-van Alphen effect was developed by Peierls,⁴ Blackman,⁵ and Landau⁶ and is based on a free-electron model. In this theory, the Schrödinger equation is solved for the case of a free-electron gas in a uniform magnetic field (H_z). The application of H_z causes the eigenvalues, the spacing and the degeneracy of the electronic energy levels to be linearly dependent on H_z . As H_z is varied, the electrons are redistributed among these H_z -dependent, quantized levels in such a way as to give rise to an oscillatory behavior. The resulting equation⁶ for the magnetic susceptibility (χ) based on a free-electron model can be expressed in the form:

$$\chi = \sum_j \left[\chi_0(H, T, \beta_j^*, E_{0j}) + \chi_1(H, T, \beta_j^*, E_{0j}) \right. \\ \left. \times \sum_{p=1}^{\infty} \frac{(-1)^{p+1} \sin[(2\pi p E_{0j} / \beta_j^* H) + \phi_j]}{2p^3 \sinh(2\pi^2 p k T / \beta_j^* H)} \right], \quad (1)$$

assuming that $E_{0j} \gg \beta_j^* H$ (or $n \gg 1$, where n is the number of occupied levels) and $E_{0j} \gg kT$. The quantity j represents the number of quadratic constant-energy

surfaces, which comprise the effective part of the highest-filled Fermi surface of constant energy with energy value E_0 . E_{0j} is the energy value of the j th highest-filled quadratic surface; for the free-electron case, $j=1$ since the Fermi surface is a single spherical surface so that $E_{0j}=E_0$. The index p is the summation index for the damped harmonics; χ_0 is the normal susceptibility, which is not a function of H and T for the free-electron case; χ_1 is the undamped amplitude of the susceptibility oscillations, which have a damped sinusoidal periodicity (of period β_j^*/pE_{0j}) in H^{-1} . ϕ_j is the phase of the damped sinusoidal oscillations of the j th quadratic surface and is equal to $\pi/4$ for the free-electron case. $\beta_j^* = e\hbar/m_j^*c$ is the effective double Bohr magneton for the j th quadratic surface, where m_j^* is the effective mass parameter. For a spherical surface, m_j^* is an isotropic, energy-independent parameter (in the free-electron case, $m_j^*=m_0$, where m_0 is the free-electron mass). For an ellipsoidal surface, m_j^* becomes an anisotropic, energy-independent parameter by the Blackman transformation.⁵ For nonquadratic surfaces, the theory becomes more complicated,^{7,8} since m^* is no longer an energy-independent parameter.

Upon substituting parameters for the alkali and noble metals into Eq. (1), it is found that the observance of an oscillatory behavior for these nearly-free electron metals would be very difficult. However, the de Haas-van Alphen effect has been observed experimentally in bismuth and fourteen other metallic single crystals.⁹ In order to apply the theory of the de Haas-van Alphen effect in real metals, the periodic potential of the lattice must be taken into account. Jones¹⁰ has shown that the anomalous properties of bismuth can be explained on a model where the highest filled Fermi surface of constant energy overlaps the energy gap at the prominent Brillouin zone boundary into the next higher zone in some directions of \mathbf{k} space. This overlapping forms electronic conduction bands and also leaves unfilled regions within the prominent zone in other directions of \mathbf{k} space, which forms hole conduction bands. From the trigonal symmetry of bismuth, Jones represents these overlapping surfaces by three identical ellipsoidal surfaces of constant energy, which can be transformed into one another by a rotation of plus or minus 120° about the trigonal axis. The E_{0j} for the overlapping electronic ellipsoids are measured upwards from the bottom of the higher zone. The E_{0j} for the unfilled hole surfaces is measured downwards from the top of the prominent zone. The E vs k curves for the overlapping electrons have high curvatures which result in a low m_j^* and correspondingly a high β_j^* .

² L. Schubnikow and W. J. de Haas, Leiden Comm. No. 207d (1930).

³ W. J. de Haas and P. M. van Alphen, Leiden Comm. No. 212A (1930).

⁴ R. Peierls, Z. Physik **81**, 186 (1933).

⁵ M. Blackman, Proc. Roy. Soc. (London) **A166**, 1 (1938).

⁶ L. D. Landau, see appendix of reference 9 (1939).

⁷ P. G. Harper, Proc. Phys. Soc. (London) **A68**, 874 (1955).

⁸ I. M. Lifshitz and A. M. Kosevich, J. Exptl. Theoret. Phys. U.S.S.R. **29**, 730 (1955) [translation: Soviet Phys. JETP **2**, 636 (1956)].

⁹ D. Shoenberg, Trans. Roy. Soc. (London) **245**, 1 (1952).

A review article on the de Haas-van Alphen effect with an extensive bibliography of the work up to 1952.

¹⁰ H. Jones, Proc. Roy. Soc. (London) **A147**, 396 (1934).

Also, the E_{0j} for the overlapping ellipsoids are very small. These conditions of a high β_j^* and a low E_{0j} favor the easy detection of the de Haas-van Alphen effect.

In 1939, Shoenberg¹¹ made a detailed de Haas-van Alphen investigation for bismuth, which showed that the three overlapping-ellipsoid model for the electronic conduction band was applicable. For an arbitrary orientation of the magnetic field with respect to the crystalline axes, three periods of oscillation were observed to be superimposed upon each other. Each of the three ellipsoids contributed one oscillatory term to the j summation in Eq. (1). Good agreement between theory and experiment was obtained by treating β_j^* and E_{0j} as adjustable parameters. Since no oscillatory evidence was found that could be attributed to the hole conduction band, its effect must be negligible compared to that of the electronic conduction band. Shoenberg also found that the principal axes of the ellipsoids were not coincident with the crystalline axes. Instead, the principal axes of each ellipsoid were rotated by an angle (θ) about one of the three corresponding binary axes. This tilted, three ellipsoid model has been shown to be applicable to antimony⁹ and arsenic¹² as well, and henceforth will be referred to as the Jones-Shoenberg (J-S) model.

In 1953, correlations^{13,14} were established between the period of the susceptibility oscillations for an oriented bismuth single crystal and the period of similar oscillations in the transverse magnetoresistance for the same bismuth crystal at the same orientation with respect to the magnetic field. This correlation was further verified for the Hall effect,^{15,16} the magnetothermoelectric effect^{17,18} and the magnetothermal conductivity^{17,19} of bismuth. This correlation was also extended to some of the other de Haas-van Alphen metals, such as graphite,^{20,21} zinc,^{20,22,23} tin²⁴ and antimony.²⁵ The one-to-one correspondence between the periods (β_j^*/E_{0j} in H^{-1}) of the de Haas-van Alphen effect and of the oscillatory galvanomagnetic and thermomagnetic effects in transverse magnetic fields has now been established on an experimental basis. Davydov and Pomeranchuk²⁶ give a theoretical basis for the oscillatory magneto-

resistance of bismuth. Recently, Zil'berman²⁷ has given a more general, theoretical basis for oscillatory galvanomagnetic and thermomagnetic effects in which the resulting equations have the same form, in essence, as the resulting equations of the de Haas-van Alphen theory. Thus, from the above experimental and theoretical bases, it is assumed in this paper that the susceptibility (χ) terms in the de Haas-van Alphen equations can be replaced to a fair approximation by corresponding galvanomagnetic terms in the analysis of oscillatory galvanomagnetic effects.

The effects of variables other than the magnetic field on the de Haas-van Alphen parameters have also been studied. For examples, the effect of pressure on the Hall effect of bismuth^{28,29} and of temperature on the susceptibility of zinc^{30,31} has been investigated. Although Steele²⁵ found an oscillatory behavior for the galvanomagnetic effects of antimony in H_T in the vicinity of 25 000 gauss, he did not find an oscillatory behavior for the galvanomagnetic effects^{32,33} in H_L up to 60 000 gauss. This failure to observe a magneto-oscillatory behavior in H_L raised the question as to whether the direction of J had a strong effect on the oscillatory galvanomagnetic phenomena. Since bismuth exhibits a more pronounced magneto-oscillatory behavior than antimony in H_T , experiments to search for the existence of a magneto-oscillatory behavior in H_L on oriented bismuth single crystals became desirable.

In order to avoid beats between the three oscillatory terms of the J-S model, the following two oriented single crystals were selected for study:

(a) \mathbf{H} parallel to the trigonal axis and therefore perpendicular to all three binary axes. In this case, the three periods are all equal so that only one period of oscillation should be observed. In addition for electrical measurements, \mathbf{H} is parallel to both \mathbf{J} and the crystal length as shown in Fig. 1.

(b) \mathbf{H} perpendicular to the trigonal axis and parallel to one of the three binary axes. In this case, there are two equal long periods with large amplitudes and one short period with a small amplitude, so that only the long period oscillation should be predominantly observed. Also, \mathbf{H} is parallel to both \mathbf{J} and the crystal length as shown in Fig. 2.

The normal galvanomagnetic effects in H_L can be shown to exist for anisotropic conductors from a model

¹¹ D. Shoenberg, Proc. Roy. Soc. (London) **A170**, 341 (1939).

¹² T. G. Berlincourt, Phys. Rev. **99**, 1716 (1955).

¹³ P. B. Alers and R. T. Webber, Phys. Rev. **91**, 1060 (1953).

¹⁴ T. G. Berlincourt, Phys. Rev. **91**, 1277 (1953).

¹⁵ L. C. Brodie, Phys. Rev. **93**, 935 (1954).

¹⁶ Reynolds, Leinhardt, and Hemstreet, Phys. Rev. **93**, 247 (1954).

¹⁷ M. C. Steele and J. Babiskin, Phys. Rev. **98**, 359 (1955).

¹⁸ M. C. Steele and J. Babiskin, Phys. Rev. **94**, 1394 (1954).

¹⁹ J. Babiskin and M. C. Steele, Phys. Rev. **96**, 822(A) (1954).

²⁰ T. G. Berlincourt and J. K. Logan, Phys. Rev. **93**, 348 (1954).

²¹ T. G. Berlincourt and M. C. Steele, Phys. Rev. **98**, 956 (1955).

²² N. M. Nachimovich, J. Phys. (U.S.S.R.) **6**, 111 (1942).

²³ P. B. Alers, Phys. Rev. **101**, 41 (1956).

²⁴ P. B. Alers, Bull. Am. Phys. Soc. Ser. II, **1**, 116 (1956).

²⁵ M. C. Steele, Phys. Rev. **99**, 1751 (1955).

²⁶ B. Davydov and I. Pomeranchuk, J. Phys. (U.S.S.R.) **2**, 147 (1940).

²⁷ G. E. Zil'berman, J. Exp. Theoret. Phys. U.S.S.R. **29**, 762 (1955) [translation: Soviet Phys. JETP **2**, 650 (1956)].

²⁸ W. C. Overton, Jr., and T. G. Berlincourt, Phys. Rev. **99**, 1165 (1955).

²⁹ N. E. Alexeevskii and N. B. Brandt, J. Exp. Theoret. Phys. U.S.S.R. **28**, 379 (1955) [translation: Soviet Phys. JETP **1**, 384 (1955)].

³⁰ J. W. McClure and J. A. Marcus, Phys. Rev. **84**, 787 (1951).

³¹ T. G. Berlincourt and M. C. Steele, Phys. Rev. **95**, 1421 (1954).

³² M. C. Steele, Phys. Rev. **97**, 1720 (1955).

³³ M. C. Steele, *Proceedings of the Conference on Low Temperature Physics, Paris, 1955* (Centre National de la Recherche Scientifique, and UNESCO, Paris, 1956), Bull. inst. intern. froid, Suppl. 1955-3, January, 1956, p. 415.

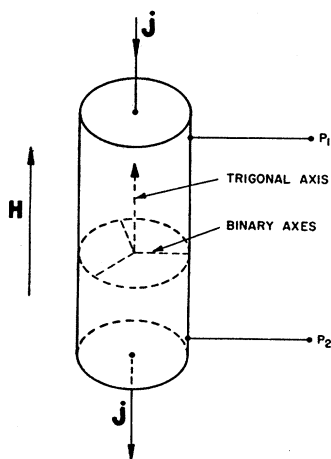


FIG. 1. Orientation and experimental arrangement for Bi I.

where the Fermi energy surface is represented by multi-ellipsoidal energy surfaces. Since a three-ellipsoid model has been shown to be applicable to the analysis of the oscillatory phenomena of bismuth,¹¹ antimony,⁹ and arsenic,¹² therefore these group V metals should be expected to exhibit interesting normal galvanomagnetic effects in H_L . Steele^{32,33} observed these effects for antimony single crystals, where the magnetic field was perpendicular to the trigonal axis and either parallel or perpendicular to a binary axis. Steele³² also observed an anomalous maximum in the longitudinal magnetoresistance, which can be qualitatively explained by the superposition of two magnetoconduction mechanisms: (a) The normal bulk magnetoresistive increase; (b) a magnetoresistive decrease in increasing magnetic fields due to decreased surface scattering. The second mechanism was proposed by MacDonald³⁴ for experiments with thin sodium wires which showed a magnetoresistive decrease. In view of the above, it seemed reasonable to study the normal galvanomagnetic effects in H_L for oriented bismuth single crystals in order to determine whether the anomalous behavior for antimony was common to the group V metals.

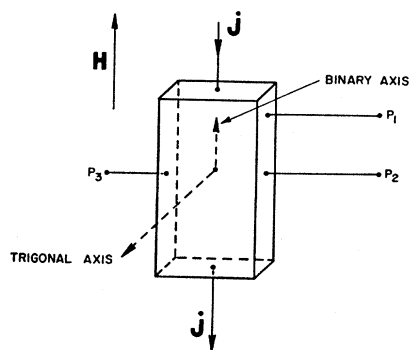


FIG. 2. Orientation and experimental arrangement for Bi II.

EXPERIMENTAL DETAILS

Oriented single crystals of outgassed 99.99% pure bismuth (Cerro de Pasco Copper Company) were grown by a seeding technique on a modified Schubnikow³⁵ furnace. Since bismuth expands upon solidification, the bismuth was formed into the desired shape and size between movable Pyrex glass plates in order to prevent strains, which would be caused by a rigid mold. Silicone oil prevented the bismuth from sticking to the glass. The seeded specimens had either a $\frac{3}{16}$ -in. diameter circular cross section or a 0.050-in. \times $\frac{1}{4}$ -in. rectangular cross section and were determined to be single crystals by etching in dilute nitric acid. The orientation was determined on a two circle goniometer by the reflection of light patterns from the etch pits of the three binary axes. The desired orientations shown in Figs. 1 and 2 were obtained to within 1.5° . Current and potential probes were attached to the crystals at the positions shown in Figs. 1 and 2 with a low melting (55°C) solder. The distance between the potential probes ranged from $\frac{1}{2}$ in. to $\frac{3}{4}$ in. The crystal was aligned with respect to the magnetic field to within 1° .

Magnetic fields continuously variable to 60 000 gauss were provided by a Bitter³⁶ solenoid and were controllable to 0.1%. The magnet calibration was known to 1% and the field was uniform to within 1% over the crystal. Although the experiments were performed mainly in the liquid helium temperature range from 1.2°K to 4.2°K, some experiments were also performed at 300°K and at liquid (78°K) and solid (47°K) nitrogen temperatures.

The measurements were taken on a 10-millivolt X - Y recorder. The magnetic field which is directly proportional to the magnet current was recorded on the X -axis by measuring the voltage across a known resistance in series with the magnet. The magnetic field was varied continuously throughout its entire range, so that all the data presented are continuous. The voltage across the potential probes of the bismuth specimens was recorded on the Y -axis, after being appropriately amplified by a Leeds and Northrup Stabilized dc Microvolt Amplifier. The bismuth current was held constant to better than 0.1%. Figure 3 exhibits a typical X - Y recorder trace. When more detailed, continuous data were necessary for analytical purposes, each one-millivolt square on the X - Y recorder trace containing data was amplified by a factor of 10 to full scale in both the X and Y directions.

EXPERIMENTAL RESULTS

A. Bi I

Figure 1 shows a schematic drawing of the experimental arrangement for the first crystal orientation studied, which will hereafter be referred to as Bi I.

³⁴ D. K. C. MacDonald, *Nature* **163**, 637 (1949).

³⁵ L. Schubnikow, *Leiden Comm. No. 207b* (1930).

³⁶ F. Bitter, *Rev. Sci. Instr.* **10**, 373 (1939).

The crystal length, \mathbf{H} and \mathbf{J} were all parallel to the trigonal axis and perpendicular to the three binary axes. P_1 and P_2 are potential probes for longitudinal magnetoresistance measurements. Bi I had an approximately circular cross-section and a 0.008 resistance ratio from 4.2°K to 300°K. The results for Bi I were reproducible from one experiment to another.

Figure 3 shows a typical X-Y recorder trace at 1.2°K, where the full scale of the Y-axis is 500 microvolts. \mathbf{J} was 140 milliamperes for all the liquid helium experiments on Bi I. The existence of an oscillatory dependence superimposed on the longitudinal magnetoresistance is clearly seen. In addition, a short-period oscillatory component is superimposed on the main long-period oscillation at the higher magnetic fields. The initial negative magnetoresistance might be attributed to a size effect.³⁴

Experiments were also performed at 3°K and 4.2°K, which indicated the same typical behavior as the 1.2°K data. The amplitude of the long-period oscillation decreased with increasing temperatures as indicated in Eq. (1). The amplitude of the short-period oscillation became vanishingly small at 4.2°K, in which case the long-period oscillation exhibited the expected single period of oscillation.

Figure 4 shows a plot of the change in resistance of Bi I in H_L at 47°K, 78°K and 300°K. These data are qualitatively similar to those obtained in the following two experiments:

(a) the temperature dependence of the de Haas-Alphen effect for zinc,³¹ in which the period of oscillation was observed to spread out progressively as the temperature was increased from 4.2°K to 300°K. In Fig. 4, the spreading of the maximum and minimum of the 47°K data at higher temperatures is suggestive of such a temperature-dependent period of oscillation.

(b) The temperature dependence of the longitudinal magnetoresistance of antimony³² in which the position of an anomalous resistance maximum was observed to shift to higher fields at higher temperatures as in Fig. 4, but no minimum was observed as in the present 47°K data. Further data between 4.2°K and 47°K would be necessary in order to make a logical choice as to which one of these two similarities is more applicable.

An experiment was also performed on Bi I at 4.2°K in order to determine whether the magnitude of \mathbf{J} had any effect on the period of oscillation. The current was varied by a factor of 200 (from 0.2 to 40 milliamperes) with no observable difference in the magneto-oscillatory characteristics, and with no departures from Ohm's law.

B. Bi II

Figure 2 shows a schematic drawing of the second crystal orientation studied, hereafter referred to as Bi II. The crystal length, \mathbf{H} and \mathbf{J} were all parallel to a binary axis and perpendicular to the trigonal axis. P_1 , P_2 and P_3 are potential probes. The longitudinal

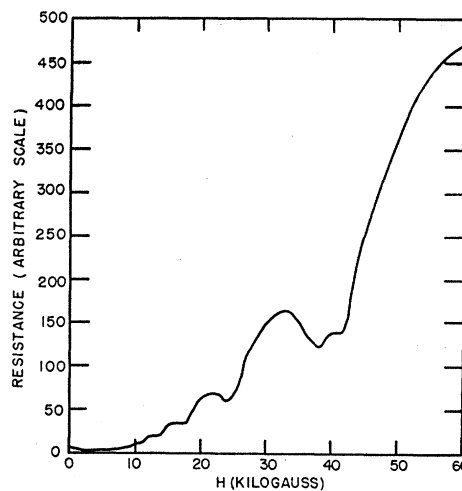


FIG. 3. Longitudinal magnetoresistance for Bi I at 1.2°K as traced from a typical X-Y recorder plot.

magnetoresistance is measured across P_1 and P_2 . Transverse voltages in H_L are measured across P_2 and P_3 . Bi II had a rectangular cross section and a 0.003 resistance ratio from 4.2°K to 300°K, which is comparable to the best crystals reported.¹¹

Figure 5 shows some of the 4.2°K data for the longitudinal magnetoresistance of Bi II with a measuring current of 2 amperes. Curve I shows the result for the first experiment performed on Bi II and exhibits three phenomena:

(a) The normal longitudinal magnetoresistance, which exhibits an anomalous resistance maximum similar to that observed by Steele³² in antimony for this orientation.

(b) At low fields, a long-period oscillatory behavior is superimposed on the normal longitudinal magnetoresistance. This long-period oscillation is the predominant single period described in the Introduction for this orientation. Calculations show that the oscillatory

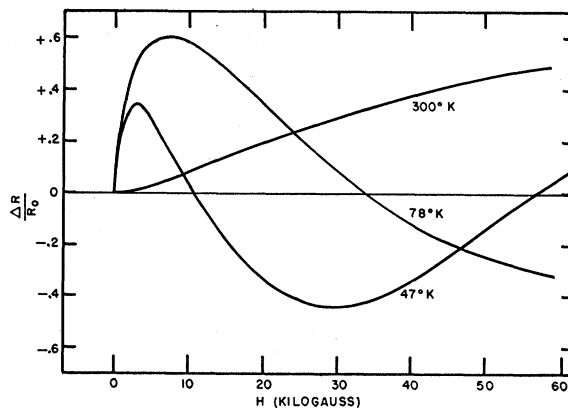


FIG. 4. Temperature dependence of the change in resistance for the longitudinal magnetoresistance of Bi I.

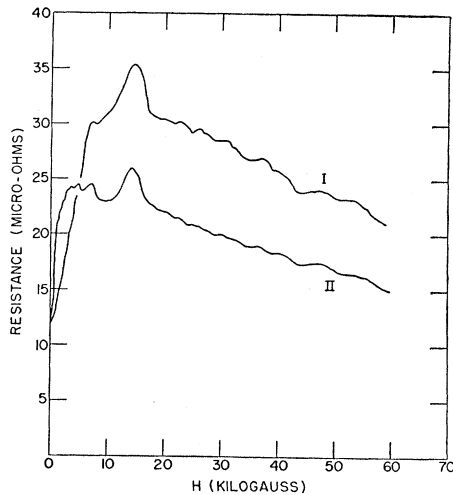


FIG. 5. Longitudinal magnetoresistance for Bi II at 4.2°K. Curves I and II show the results, respectively, for the first and second experiments.

maximum at 15 000 gauss is the last oscillatory maximum possible.

(c) At high fields, after the last possible long-period oscillation, a short-period oscillatory behavior was observed, which could not be clearly resolved due to experimental difficulties encountered at the higher fields.

Curve II of Fig. 5 shows the result of a second experiment on Bi II. Even though the resistance ratio from 4.2°K at $H=0$ of Curve II did not differ appreciably from that of Curve I, the galvanomagnetic properties of Curve II did not reproduce those of Curve I. This nonreproducibility was most probably due to strains induced by the thermal shock of cycling between 4.2°K and 300°K. Although Curve II exhibits the same general features as Curve I, the anomalous resistance maximum shifted to a lower magnetic field and the short-period oscillation at the high fields was observed more clearly. In succeeding experiments the galvanomagnetic properties of Bi II deteriorated progressively with the resistance maximum shifting to very low magnetic fields and all the oscillatory behavior disappearing.

Experiments were also performed at room temperature and liquid nitrogen temperatures, in which the resistance maximum shifted to higher magnetic fields as the temperature increased. This is the same type of behavior observed for antimony.³² However, none of these data are presented here, due to the progressive deterioration of the galvanomagnetic properties between experiments.

A typical result for the transverse voltage measured across P_2 and P_3 in H_L at 4.2°K is shown in Fig. 6. This voltage changed sign as H_L increased and exhibits only a slight oscillatory dependence. The existence of the voltage at $H=0$ is probably due to a slight misalignment of the potential probes. No unambiguous

explanation for the anomalous behavior at the very lowest magnetic fields can be offered at this time.

DISCUSSION AND ANALYSIS

A. Periodic Oscillations in Bi I

From Eq. (1), the oscillations are periodic in H^{-1} . Therefore, a table of 230 points having equal increments in H^{-1} was prepared for the reduction of the detailed, continuous data from the $X-Y$ recorder. The upper graph of Fig. 7 shows a plot of the longitudinal magnetoresistance for Bi I against H^{-1} for the 4.2°K data. The central dashed curve of the upper graph is the mean about which the experimental data oscillate periodically. This mean is determined graphically from the upper and lower dashed envelope curves drawn tangent to the experimental data. The difference between the mean dashed curve and the experimental data is plotted on the lower graph. The period of the oscillations is determined from the distance between the nodes.

The nodal period of these data is $\beta_j^*/E_{0j} = 1.58 \times 10^{-5}$ gauss⁻¹. This period is in excellent agreement with the value of 1.57×10^{-5} gauss⁻¹ obtained by Overton and Berlincourt²⁸ in measurements of the transverse magnetoresistance and Hall effect of bismuth. A comparison of the orientation for their transverse magnetoresistance measurements and the above longitudinal magnetoresistance measurements shows the following:

- (a) \mathbf{H} was parallel to the trigonal axis in both measurements;
- (b) $\mathbf{H} \perp \mathbf{J}$ for the transverse magnetoresistance measurements, but $\mathbf{H} \parallel \mathbf{J}$ for the longitudinal magnetoresistance measurements.

The excellent agreement between the above results shows that the period of oscillation is independent of the direction of \mathbf{J} and its associated electric field. It was also shown above in the experimental results for Bi I that the period was independent of the magnitude of \mathbf{J} as well, where Ohm's law was still obeyed. Therefore,

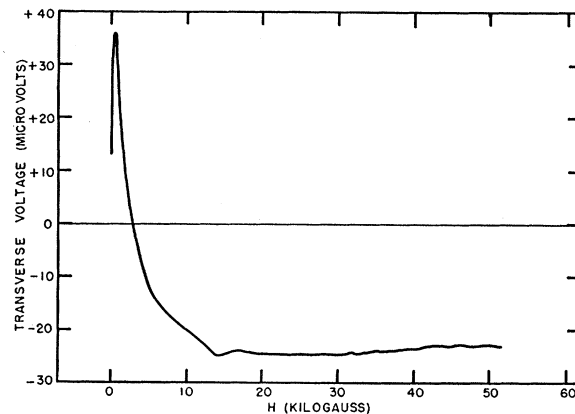


FIG. 6. Transverse voltage in a longitudinal magnetic field for Bi II at 4.2°K.

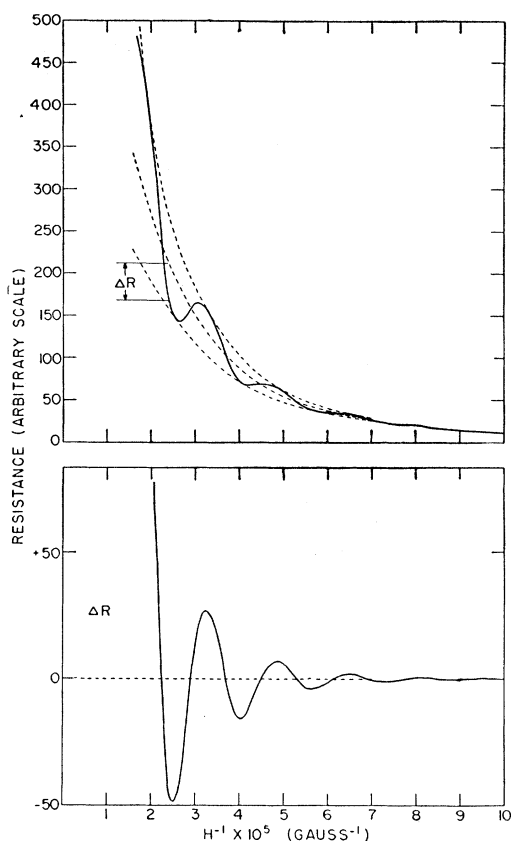


FIG. 7. Longitudinal magnetoresistance for Bi I at 4.2°K plotted against reciprocal magnetic fields (H^{-1}). The lower figure shows ΔR plotted on an expanded scale.

the conclusion can be drawn from these results that the periods of oscillatory galvanomagnetic phenomena depend to first order solely upon the orientation of \mathbf{H} with respect to the crystalline axes.

When one uses Shoenberg's parameters⁹ which are obtained from the fitting of the de Haas-van Alphen data to the J-S model, the calculated value of the three equal periods for this orientation is 1.17×10^{-5} gauss⁻¹. This disagreement for this particular orientation between the calculated de Haas-van Alphen period and the observed galvanomagnetic periods is not too surprising, since actual de Haas-van Alphen measurements using Shoenberg's torsion balance cannot be performed at this orientation. The extrapolation of the de Haas-van Alphen measurements to this orientation could easily be in error. In fact, Shoenberg¹¹ states that some of the parameters, which are approximated from data fitting, could be in error by as much as 25%.

Since oscillatory galvanomagnetic effects are actually observed at this orientation, the observed period of 1.58×10^{-5} gauss⁻¹ is believed to be more reliable than the calculated period of 1.17×10^{-5} gauss⁻¹. This belief is supported by the most recent cyclotron resonance

measurements³⁷ at this orientation, which give an electronic $m_j^* = 0.04m_0$ instead of the $m_j^* = 0.055m_0$ obtained for Shoenberg's parameters. With the reasonable assumption that Shoenberg's value for E_{0j} is correct, this $m_j^* = 0.04m_0$ leads to a value of $\beta_j^*/E_{0j} = 1.61 \times 10^{-5}$ gauss⁻¹ which is in good agreement with the above observed results. Furthermore this disagreement is inconsistent with the observed one-to-one correspondence between the periods of the de Haas-van Alphen and oscillatory galvanomagnetic effects at other orientations.

In addition to the above main period of oscillation, a short-period oscillation was also observed for Bi I. This short period is of the order of eight times smaller than the main period and is seen clearly in Figs. 3 and 8 at the higher fields and lower temperatures. Periods other than the main period could arise from the higher order, damped harmonics in Eq. (1), or from beats between the main three periods due to misalignment, or from holes. The reasons for discounting the possibility of attributing the short period to the higher order, damped harmonics will be given shortly. An examination of the short period revealed that its amplitude was not monotonically damped in H^{-1} , but rather that it had the characteristics of a beat period. Thus the short period is attributed to beats arising from a very slight misalignment of \mathbf{H} with respect to the trigonal axis.

In the present and previous experiments on bismuth, no oscillatory behavior was found which could be attributed to holes. If the energy surfaces for the holes could be represented by quadratic surfaces, then this failure to observe holes can be simply explained on the

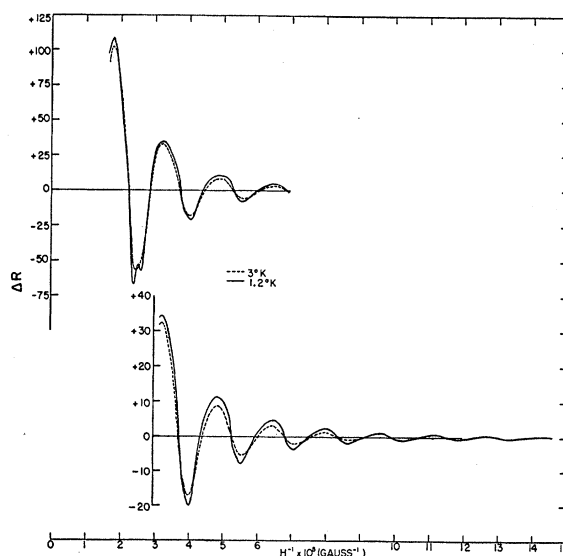


FIG. 8. ΔR for the longitudinal magnetoresistance of Bi I at 1.2°K and 3°K plotted against reciprocal magnetic fields (H^{-1}). The lower figure gives the lower magnetic-field data plotted on an expanded ΔR scale.

³⁷ Lax, Button, Zeiger, and Roth, Phys. Rev. **102**, 715 (1956). Also, J. K. Galt (private communication).

basis that its periods were too small to be measured. This would be true, if the m_j^* and E_{0j} for the holes were considerably greater than those for the electrons. This surmise is substantiated in cyclotron resonance measurements by Galt *et al.*³⁸ who find that heavy holes with $m^*=0.3m_0$ are the majority carriers. Galt also reports a very light hole mass, which would give rise to an easily observable oscillatory behavior. However, the cyclotron resonance associated with this light hole has since been shown to be attributable^{37,39} to other causes. The failure to observe an oscillatory behavior for holes can also be explained, if the energy surfaces for the holes were warped. In this case,⁷ m_j^* is no longer an energy-independent parameter and the sharp, degenerate levels associated with oscillatory phenomena are drawn out into bands of varying widths. If these bands are sufficiently broad, they will overlap and the oscillatory phenomena will become negligible.

B. Departures from Nodal Periodicity in Bi I

It was noted in the high field data of Fig. 7 at 4.2°K that the distance between the nodes of last half-period oscillation below the ΔR axis was 20 percent smaller than the value of $\beta_j^*/2E_{0j}=0.79 \times 10^{-5}$ gauss⁻¹ given above. This departure from periodicity was much too large to be attributed to errors in drawing the envelope curves. Therefore, it was believed at first to be due to an unexplained high-field compression of the period.

The reason for this discrepancy became apparent upon plotting the 1.2°K and 3°K data, which are shown in Fig. 8 as a plot of ΔR against H^{-1} . Two observations concerning nodal periodicity were noted:

(a) Each complete oscillation exhibited nodal periodicity in H^{-1} at the lower fields and higher tempera-

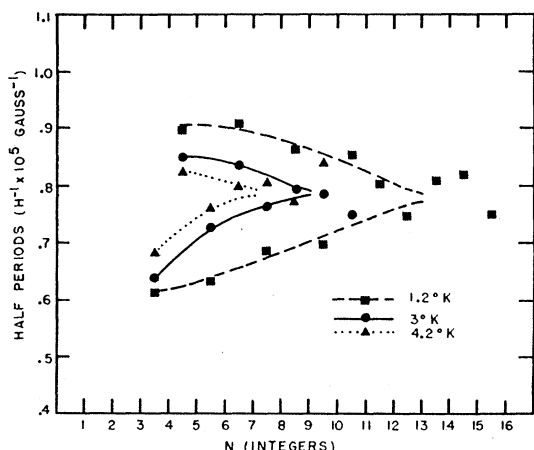


FIG. 9. Departures from nodal periodicity for Bi I. The half-period distance between nodes is plotted against integers representing the nodes. Note that the points are plotted midway between the integers.

³⁸ Galt, Yager, Merritt, Getlin, and Dail, *Phys. Rev.* **100**, 748 (1955).

³⁹ M. Tinkham, *Phys. Rev.* **101**, 902 (1956).

tures, but exhibited only an approximate nodal periodicity at the higher fields and lower temperatures.

(b) Although the half-oscillations exhibited nodal periodicity in H^{-1} as predicted in Eq. (1) at the lower fields and higher temperatures, they systematically exhibited progressively larger departures from nodal periodicity at the higher fields and lower temperatures. The nodal half-periods became progressively greater than $\beta_j^*/2E_{0j}$ for the half-oscillations above the ΔR axis and progressively smaller than $\beta_j^*/2E_{0j}$ for the half-oscillations below the ΔR axis.

In order to emphasize the nature of this effect, Fig. 9 shows a plot of the distances between the nodes of the half-period oscillations of the ΔR curves against integers representing the nodes at 1.2°K, 3°K and 4.2°K. By the graphical extrapolation of Fig. 8 to higher fields, nodes were calculated to exist at $\sim 75\,000$ gauss and a last possible node at $\sim 150\,000$ gauss. Therefore, the highest field node in Fig. 8 is the third node and the half-period length between the third and fourth nodes is the first point in Fig. 9. The gradual change from the periodic nodal distances at the lower fields and higher temperatures to the nonperiodic nodal distances at the higher fields and lower temperatures is apparent from the schematic curves in Fig. 9. Since the nodal distances at the higher fields and lower temperatures are not periodic, the oscillatory data cannot be analyzed simply in terms of the monotonically damped harmonics of Eq. (1).

These departures from nodal periodicity can be qualitatively explained on the basis that Eq. (1) is no longer an accurate representation of the behavior of oscillatory phenomena without the assumption for $n \gg 1$ or $E_{0j} \gg \beta_j^* H$. When H is sufficiently large so that only a small number of quantum levels are occupied, the summation in the determination of the partition function can now be summed term by term,⁴ rather than being expressed⁶ by a Poisson summation formula in order to obtain Eq. (1). Upon summing term by term, an exact expression for the diamagnetic moment of a free-electron gas at 0°K is obtained and is exhibited as a function of H by Peierls⁴ and in two other sources,^{40,41} which show the alternately short and long half-periods. If the exact diamagnetic moment were nodally periodic in H^{-1} , then these plots against H should have exhibited progressively longer half-periods in increasing H . The cusps in these figures occur each time in decreasing magnetic fields that a previously unoccupied energy level starts to become occupied. A plot of the exact diamagnetic moment for a free-electron gas against H^{-1} appears in some unpublished work of de Launay,⁴² which clearly exhibits the alternately long and short

⁴⁰ N. F. Mott and H. Jones, *Theory of the Properties of Metals and Alloys* (Oxford University Press, London, England, 1936), p. 216.

⁴¹ F. Seitz, *The Modern Theory of Solids* (McGraw-Hill, New York, 1940), p. 500.

⁴² J. R. de Launay (private communication).

half-oscillations and also the approximate periodicity of the complete oscillations. The exact theory does not contain any harmonic terms as does Eq. (1) and does not exhibit nodal periodicity. The behavior predicted by the free-electron theory is highly similar to Fig. 8 in which it can be shown that there are only two occupied quantized levels present for the last observed high-field oscillation. For $T > 0^\circ\text{K}$, the cusps at 0°K are smoothed due to the spreading of the energy levels, so that the oscillations approximate the sinusoidal periodicity of Eq. (1) more closely. Since neither the experimental data nor the exact theory exhibited nodal periodicity for $n \gg 1$, the possibility of explaining the short (beat) period of Bi I as the eighth harmonic of the main period can be discounted. These reasons also explain why the more predominant harmonics (such as the second and third harmonics) did not appear in the experimental results.

This correlation between the exact theoretical oscillatory diamagnetic moment for a free-electron gas and

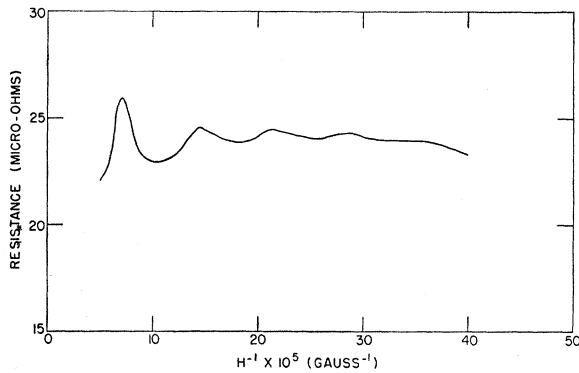


FIG. 10. Long-period oscillation for Bi II at 4.2°K plotted against reciprocal magnetic fields (H^{-1}).

the observed oscillatory galvanomagnetic phenomena for a real metal with overlapping bands is rather remarkable. If the oscillatory effects of the hole surfaces are neglected as is justified from an experimental standpoint, the oscillatory effects of the three electronic ellipsoids can be simply added for the orientation of Bi I, so that the over-all effect would be similar to that of a single ellipsoid. Thus it is seen that the choice of crystal orientation, so that only one period is predominantly observed, has served to show this correlation clearly. This correlation lends strong support for the validity of the J-S model. A probable explanation of this correlation is that the density of states and the E vs k curves at the bottom of an overlapping electronic conduction band have a parabolic dependence, as in the free-electron case. Therefore, the introduction of an energy-independent m_j^* is a valid approximation. This explanation is applicable to bismuth, since the E_{0j} for the very small number of electrons in the overlapping electronic conduction bands are only 0.018 ev .⁹ How-

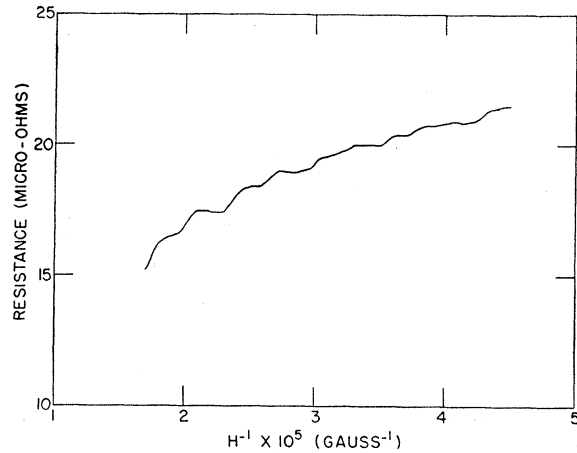


FIG. 11. Short-period oscillation for Bi II at 4.2°K plotted against reciprocal magnetic fields (H^{-1}).

ever, in the absence of a detailed theory for the oscillatory galvanomagnetic effects, one cannot exclude the possibility that this seemingly reasonable correlation is just coincidental.

C. Periodic Oscillations in Bi II

Two oscillatory behaviors were observed in Fig. 5. A long-period oscillation at low fields and a short-period oscillation at high fields. The amplitude of the short-period oscillation is too small to be observed at low fields and it only appears at the high fields after the long-period oscillation has gone through its last possible oscillation. Due to the small voltages measured for Bi II, the oscillatory behavior is not as clear as for Bi I. Figure 10 is a plot of the longitudinal magnetoresistance against H^{-1} for curve II of Fig. 5 and exhibits the long-period oscillation at low fields. The period of this oscillation is $\beta_j^*/E_{0j} = 7.1 \times 10^{-5} \text{ gauss}^{-1}$. The same value was obtained for this orientation by Steele and Babiskin¹⁷ for transverse magnetoresistance and thermomagnetic effects. This excellent agreement further confirms the previous conclusion that the period of oscillation for transport phenomena does not depend on the direction of \mathbf{J} .

The calculated values of the three periods of oscillation for this orientation using the de Haas-van Alphen effect parameters given by Shoenberg⁹ are 7.1×10^{-5} , 7.1×10^{-5} , $0.25 \times 10^{-5} \text{ gauss}^{-1}$. It is seen that the periods for oscillatory transport phenomena given above are in excellent agreement with the two predominant equal long periods calculated from Shoenberg's parameters.

Figure 11 exhibits the short-period oscillation at high fields plotted against H^{-1} from curve II of Fig. 5. The period of this oscillation is $0.3 \times 10^{-5} \text{ gauss}^{-1}$, which compares favorably with the above calculated value of $0.25 \times 10^{-5} \text{ gauss}^{-1}$. The observation of this short period is a striking example of the validity of the J-S model in the analysis of the oscillatory phenomena for bismuth.

The absence of this short period in Shoenberg's¹⁴ measurements on the de Haas-van Alphen effect up to 9000 gauss and in Steele and Babiskin's¹⁷ measurements on oscillatory transport phenomena up to 13 000 gauss is not too surprising. This absence can be deduced from Eq. (1), which shows that the amplitude of short-period oscillations are more heavily damped than long period oscillations.

The condition that n is not $\gg 1$ as discussed for Bi I is also satisfied by the long period oscillation of Bi II. It is noted in Fig. 10 for Bi II at 4.2°K, that the last oscillations have alternating short and long half periods as for Bi I. A re-examination of the long period data of Steele and Babiskin¹⁷ showed that the oscillatory thermomagnetic phenomena at 1.6°K and the magnetoresistance at 1.23°K exhibited the alternating short and long half periods most clearly. In fact, the oscillatory thermomagnetic phenomena exhibited a pronounced cusp-like behavior. These observations lend further support to the correlation found for Bi I.

D. Normal Galvanomagnetic Effects

The normal galvanomagnetic effects in H_L which were observed in these experiments, are smaller than the corresponding H_T effects by orders of magnitude. Even though \mathbf{H} , \mathbf{J} , the crystal length and the appropriate crystalline axis were all aligned parallel with respect to each other to about 1°, this is not sufficient to rule out the possibility that some percentage of the observed H_L effects might be due to small H_T components arising from slight misalignments. From classical conduction models, this percentage would be 100%. However, from the application of the J-S model to the theory of magnetoconductivity, it will be shown that the H_L effects do exist, but it is still not known what percentage of the observed effects is due to H_L or to a small H_T component. The virtual absence of beat periods in the observed oscillatory galvanomagnetic effects shows that the alignments were quite good.

To analyze the H_L effects, the Boltzmann transport equation in a magnetic field must be solved. However, Wilson⁴³ states that the application of the Boltzmann transport equation to the theory of conduction in a magnetic field is no longer valid, when it becomes necessary to take into account the magnetic quantization of the electron orbits. Since the oscillatory transport phenomena are associated with this magnetic quantization, the observed normal H_L effects for bismuth can only be analyzed at very low magnetic fields where the quantization effects are negligible. In the H_L effects, the longitudinal voltage will contain a transverse component due to inaccurate placement of the potential probes. Similarly, the transverse voltage will contain a longitudinal component. Since \mathbf{H} could not be reversed in these experiments in order to separate the even and odd components of the voltages and due to the pro-

gressive deterioration of the H_L effects in Bi II, detailed measurements were not attempted in the very-low-field region. Therefore, the only remaining analysis is to show the conditions for the existence of the H_L effects.

Kaplan⁴⁴ has obtained a solution of the Boltzmann transport equation for the normal galvanomagnetic effects in an anisotropic conductor with an ellipsoidal energy surface, assuming that the relaxation time is an energy-independent parameter. Kaplan also suggests that this solution can be applied to anisotropic conductors with multi-ellipsoidal energy surfaces by summing the effects due to each of the ellipsoids, after all the ellipsoids have been transformed to a common frame of reference. Since the results for the de Haas-van Alphen effect and oscillatory galvanomagnetic effects of bismuth have been analyzed by the J-S model, the author has independently analyzed the conditions for the normal galvanomagnetic effects of bismuth at low magnetic fields by applying the Kaplan solution to the J-S model.

Applying this solution to a single ellipsoid, the Hall voltage is the only galvanomagnetic effect obtained. A single ellipsoid does not produce any transverse or longitudinal magnetoresistance or any transverse voltage in H_L . This result is independent of whether the ellipsoid is represented by a diagonal or a nondiagonal effective-mass tensor. This result is also consistent with a statement in Wilson⁴⁵ that no magnetoresistance effects exist, if all the electrons which contribute to the electric current have the same velocity. This is due to the cancellation of the effect of the magnetic field by the Hall electric field. However, for a multi-ellipsoid model, all the electrons no longer have the same velocities and magnetoresistance effects become possible.

Recently, Abeles and Meiboom⁴⁶ have independently given a thorough analysis of the galvanomagnetic properties of bismuth similar to that outlined above. They use the J-S model for the electrons except that the angle of rotation (θ) of the ellipsoids with respect to the binary axes is set equal to zero, so that the effective-mass tensors associated with the ellipsoids are diagonal. They also use a single ellipsoid for the holes with a diagonal effective-mass tensor. They obtain good agreement between this model and experiments at 80°K and 300°K in magnetic fields up to 2000 gauss.

The solutions of Abeles and Meiboom exhibit Hall voltages and transverse magnetoresistances for all crystal orientations. They also exhibit longitudinal magnetoresistances for all (except one) crystal orientations. Their solutions provide a basis for the existence of the observed longitudinal magnetoresistance of Bi II. The exception noted above, where these solutions do not

⁴⁴ J. I. Kaplan, Phys. Rev. **99**, 1808 (1955).

⁴⁵ Reference 1, p. 215.

⁴⁶ B. Abeles and S. Meiboom, Phys. Rev. **101**, 544 (1956).

⁴³ Reference 1, p. 210.

exhibit a longitudinal magnetoresistance occurs at the orientation where \mathbf{H} and \mathbf{J} are both parallel to the trigonal axis. However, this orientation is the one at which the longitudinal magnetoresistance results for Bi I were obtained. Also, these solutions do not exhibit transverse voltages in H_L for any orientation.

Thus, it is seen that the J-S model with $\theta=0$ as used by Abeles and Meiboom, does not establish the conditions for all the observed galvanomagnetic properties of bismuth at liquid helium temperatures. This $\theta=0$ model is also inconsistent with the results obtained for oscillatory phenomena, which are analyzed by the J-S model with $\theta \neq 0$. Upon applying the J-S model with $\theta \neq 0$ to the analysis of normal galvanomagnetic phenomena, a basis for the existence of the longitudinal magnetoresistance observed for Bi I and the transverse voltage in H_L observed for Bi II is established. The galvanomagnetic tensors for the J-S model with $\theta \neq 0$ will not be displayed here, since they have very recently been independently derived by Lax *et al.*³⁷ in the analysis of cyclotron absorption in bismuth. The cyclotron absorption tensors reduce to the galvanomagnetic tensors by setting the frequency equal to zero.

The necessity of the assumption that the ellipsoids are rotated about their respective binary axes is more apparent for antimony than for bismuth. The results from the de Haas-van Alphen effect show that the angle of rotation is considerably greater for antimony⁹ than for bismuth.¹¹ The role of this rotation in providing an experimental basis for transverse galvanomagnetic effects in H_L is clearly exhibited by a comparison of the above results obtained for bismuth with the results obtained by Steele³³ for antimony. For antimony, where the angle of rotation is large, the transverse voltages observed in H_L and H_T are almost equal. Whereas for bismuth, where the angle of rotation is small, the transverse voltage observed in H_L is very much smaller than in H_T .

This above discussion suggests that further experiments on the galvanomagnetic properties of bismuth and antimony in low magnetic fields at liquid helium temperatures would be profitable. The results of such experiments could probably be analyzed with the effective-mass parameters obtained from high-field measurements.

E. Anomalous Resistance Maximum

The anomalous maximum found in the longitudinal magnetoresistance of antimony by Steele³² has now been found with bismuth (Fig. 5) as well. The position of the maximum was found to be sensitive to strain. The maximum was qualitatively explained in the Introduction by the addition of a surface-scattering mechanism to the normal magnetoresistance.

The surface scattering can be attributed to either the external surfaces of the crystal or internal surfaces.⁴⁷

⁴⁷ D. K. C. MacDonald, *Phil. Mag.* **63**, 124 (1952).

From estimates of the electronic mean free path and the radius of the classical electronic orbits in a magnetic field, it was shown^{32,47} that the distance between the scattering surfaces was less than the thickness of the crystal, but greater than atomic dimensions. This suggests that the scattering is due to internal surfaces, such as slip surfaces. For bismuth, these internal surfaces would most likely occur parallel to the principal cleavage plane. The question of whether the scattering was due to external or internal surfaces could be resolved in either of the two following types of experiments: (a) experiments with varying crystal thickness, if the scattering were due to external surfaces; (b) experiments with crystals with different orientations, if the scattering were due to internal surfaces parallel to the cleavage plane. In the latter case, the orientation of the cleavage plane is varied with respect to the direction of \mathbf{J} .

In the present work, the anomalous maximum in the longitudinal magnetoresistance was exhibited by Bi II (Fig. 5), where the principal cleavage plane was parallel to the crystal length and \mathbf{J} . However, for Bi I (Fig. 3), where the principal cleavage plane was perpendicular to the crystal length and \mathbf{J} , the longitudinal magnetoresistance increased monotonically with increasing magnetic field. If the surface scattering were due to the external surfaces of the crystal, then Bi I should have exhibited the same type of resistance maximum as did Bi II. Since Bi I does not exhibit a resistance maximum, the conclusion is postulated that the magnetoresistance decrease in Bi II is associated with scattering from internal surfaces parallel to the cleavage plane.

ACKNOWLEDGMENTS

This work was done under a cooperative arrangement between The Catholic University of America and the Cryogenics Branch of the United States Naval Research Laboratory. The author takes pleasure in thanking Dr. F. T. Byrne and Dr. K. F. Herzfeld of The Catholic University for their guidance and for their permission to use these experiments as dissertation material; Dr. M. C. Steele for his stimulating guidance and encouragement throughout the progress of this work; Dr. J. I. Kaplan and Dr. T. G. Berlincourt for helpful discussions; Dr. J. R. de Launay for the use of his unpublished work; A. H. Mister and R. C. Anonsen for the operation of the magnet; and P. G. Siebenmann for his generous assistance.

APPENDIX. THREE-ELLIPSOID MODEL FOR BISMUTH

In the above discussion, rather strong experimental support was presented for the validity of a three-ellipsoid model for bismuth and for the introduction of an energy-independent m^* . Therefore, a review of this model is now outlined, which uses a slightly modified and more general approach than that given by Black-

man⁵ and Shoenberg.⁹ In order to determine β^* for an anisotropic conductor, Blackman transforms an ellipsoidal energy surface into a spherical form and then determines the effect of this transformation on a commutation relation involving the magnetic field.

The present approach deals directly with Schrödinger's equation in a uniform magnetic field represented by the vector potential $\mathbf{A} = \frac{1}{2}\mathbf{H} \times \mathbf{r}$. We can write Schrödinger's equation in the form $\mathcal{H}\psi = (E_N - E_B)\psi$. E_B is a constant energy measured from the origin of the prominent Brillouin zone to the origin of either an overlapping electronic ellipsoid or an unfilled hole ellipsoid, where E_B respectively includes or does not include the energy gap at the zone boundary. $E_B = 0$ for the free-electron case. E_N are the total values of the quantum levels. \mathcal{H} is the Hamiltonian for any one of the E_{0j} ellipsoidal energy surfaces and is expressed as:

$$\mathcal{H} = \frac{1}{2m_0} \left(\mathbf{p} + \frac{e}{2c} \mathbf{H} \times \mathbf{r} \right) \mathbf{m}^{-1} \left(\mathbf{p} + \frac{e}{2c} \mathbf{H} \times \mathbf{r} \right), \quad (2)$$

where m_0 is the free-electron mass and \mathbf{m}^{-1} is the inverse of the diagonal effective-mass tensor \mathbf{m} , which has the components $m_1 = m_{xx}/m_0$, $m_2 = m_{yy}/m_0$ and $m_3 = m_{zz}/m_0$. (For the spherical free-electron case, $m_{xx} = m_{yy} = m_{zz} = m_0$.) If we transform the x, y, z components of \mathbf{r} , such that $x = x' m_1^{-\frac{1}{2}}$, $y = y' m_2^{-\frac{1}{2}}$, $z = z' m_3^{-\frac{1}{2}}$, then the \mathbf{p} operator is automatically transformed to $p_x = m_1^{\frac{1}{2}} p'_x$, $p_y = m_2^{\frac{1}{2}} p'_y$, $p_z = m_3^{\frac{1}{2}} p'_z$. Substituting this transformation into Eq. (2), we find that \mathbf{m}^{-1} has been transformed into a unit tensor so that \mathcal{H} is now in the following spherical form:

$$\mathcal{H} = \frac{1}{2m_0} \left(\mathbf{p}' + \frac{e}{2c} \mathbf{H}' \times \mathbf{r}' \right)^2, \quad (3)$$

where

$$\mathbf{H}'^2 = \frac{\mathbf{H} \cdot \mathbf{m} \cdot \mathbf{H}}{|\mathbf{m}|} = \frac{m_1 H_x^2 + m_2 H_y^2 + m_3 H_z^2}{m_1 m_2 m_3}, \quad (4)$$

which is the same transformation on \mathbf{H} as obtained by Blackman.

Schrödinger's equation can now be solved in the same manner as in the free-electron case. With \mathbf{H} in the z direction, we get

$$E_N - E_B = \beta H_z' \left(n + \frac{1}{2} \right) + \frac{p_x'^2}{2m_0} = \beta^* H_z \left(n + \frac{1}{2} \right) + \frac{p_x^2}{2m_{zz}}, \quad (5)$$

where $\beta^* = \beta / (m_1 m_2)^{\frac{1}{2}}$. Thus it is seen that the solution for the free-electron case can be applied to real metals

with periodic potentials, when the highest-filled Fermi surface of constant energy can be represented by a multi-ellipsoidal model. The correlation between theory and experiment for the alternating long and short half periods discussed above can probably be explained with this ellipsoidal model.

In the more general case, where \mathbf{H} is at an arbitrary orientation with respect to the xyz coordinate frame with direction cosines $\alpha_x, \alpha_y, \alpha_z$, then the following expression for β^* can be defined

$$\beta^{*2} = \left(\frac{e\hbar}{m_0 c} \right)^2 \left(\frac{1}{m^*} \right)^2 = \beta^2 \frac{\alpha \mathbf{m} \alpha}{|\mathbf{m}|}, \quad (6)$$

therefore

$$\frac{1}{m^{*2}} = \frac{\alpha_x^2}{m_2 m_3} + \frac{\alpha_y^2}{m_1 m_3} + \frac{\alpha_z^2}{m_1 m_2}. \quad (7)$$

This equation for the effective mass is the same as that obtained by Shockley⁴⁸ in the determination of the cyclotron-resonance frequency.

For bismuth, we use a crystal coordinate frame where the trigonal axis is the z -axis, any one of the three binary axes is the x -axis, and the bisectrix between the other two binary axes is the y -axis. In the J-S model, the principal axes of each ellipsoid are rotated by an angle θ about its respective binary axis. For the ellipsoid which has the x -axis as the binary axis, this rotation introduces a symmetric nondiagonal component to the effective-mass tensor, which is

$$m_4 = m_{yz}/m_0 = m_{zy}/m_0 = \frac{1}{2}(m_2 - m_3) \tan 2\theta.$$

In this case, the relations given by Shoenberg⁹ for various orientations of \mathbf{H} with respect to this ellipsoid can all be represented by the following single equation which is derived from Eq. (6):

$$\beta^{*2} = \beta^2 (m_1 \alpha_x^2 + m_2 \alpha_y^2 + m_3 \alpha_z^2 + 2m_4 \alpha_y \alpha_z) / [m_1 (m_2 m_3 - m_4^2)]. \quad (8)$$

By the rotation of this ellipsoid and its associated nondiagonal effective-mass tensor about the z -axis by plus or minus 120° , relations similar to Eq. (8) were obtained for the other two ellipsoids. In the measurement of oscillatory phenomena, the quantity β_j^*/E_{0j} is determined from the period. Therefore, in the determination of β_j^* , there are five unknown parameters which are E_0, m_1, m_2, m_3 and m_4 (or θ). Shoenberg⁹ gives values for these parameters from de Haas-van Alphen effect measurements.

⁴⁸ W. Shockley, Phys. Rev. **90**, 491 (1953).